Supplement to

Reconciling online and offline source apportionment of brown carbon absorption in wintertime Seoul

Hwajin Kim et al. — Correspondence: khj0116@snu.ac.kr

This Supplement contains the extended methods, source-apportionment and regression diagnostics, and supporting composition/optical results referenced in the main text.

Contents and main-text / Supplement allocation

Location	Content	Item
SI	Offline-AMS extraction and water-soluble OA quantification (WSOA = WSOC × OM:OC)	Table S1
SI	Online↔offline factor spectral-similarity (R^2) matrix	Table S2
SI	Regression diagnostics: MAC ± 95 % CI, VIF, condition number, NNLS refit	Table S3
SI	BC-correction sensitivity (AAEBC, reference wavelength)	Table S4
SI	Reported OA source-apportionment mass fractions underlying main-text Table 2 (Option-B weighting)	Table S5
SI	Selection of the six-factor online PMF solution: five-, six- and seven-factor spectra and time series	Fig. S1
SI	PMF diagnostics: SNR, Q/Qexp vs p, Q vs fPeak, explained variation	Fig. S2
SI	Selection of the four-factor offline PMF solution	Fig. S3
SI	Online–offline validation: PM_1 vs $PM_{2.5}$ OC/OA/WSOA and BrC absorption (370 vs 365 nm)	Fig. S4
SI	Online vs offline MO-OOA correspondence (r = 0.93; same-factor test)	Fig. S5
SI	Mean diurnal cycles of the secondary OA factors	Fig. S6
SI	Reduced-nitrogen (imidazole-type) chromophores in the online factors; NIST reference spectra	Fig. S7
SI	Online–offline factor time-series comparison for the four water-soluble factors	Fig. S8
SI	Offline water-soluble MAE365 versus the earlier Seoul record and the WS BrC literature	Fig. S9

S1 Measurement and analysis details

S1.1 Online instrumentation and BrC from the aethalometer

Non-refractory PM_1 composition was measured with an Aerodyne HR-ToF-AMS; elemental ratios used the Improved-Ambient method (Canagaratna et al., 2015). Seven-wavelength absorption was measured with an AE33 aethalometer. The AMS was operated in the same configuration as our previous Seoul campaigns (Kim et al., 2017): a 600 °C tungsten vaporizer with 70 eV electron ionization, alternating V- and W-mode, data saved at 2.5 min resolution, and non-refractory PM_1 mass quantified with a time-resolved, composition-dependent collection efficiency following Middlebrook et al. (2012). The AE33 sampled at 5 L min^{-1} behind the same $PM_{2.5}$ inlet, onto M8060 filter tape (spot area 0.785 cm^2) at a 1 min time base, with the dual-spot loading compensation applied internally. Brown-carbon absorption was then isolated as babs,BrC(λ) = babs(λ) − babs(880 nm) × (λ/880)^(−AAEBC), taking 880 nm as the BC reference band and AAEBC = 1.0. This choice sets the absolute BrC level but not the attribution: over AAEBC = 0.9–1.1 and reference bands of 880 or 950 nm the 370 nm BrC fraction moves from its base value of 25.7 % to between 18.4 % and 32.4 % — about ±6–7 % absolute — while the online source ranking is unchanged in every case (Table S4, Sect. S2.2).

S1.2 Offline-AMS protocol

The 24 h $PM_{2.5}$ quartz filters were analysed by offline-AMS: water extraction, argon nebulisation, drying, and HR-ToF-AMS detection, following the protocol of Daellenbach et al. (2016) and its argon implementation by Bozzetti et al. (2017). The water-soluble organic aerosol mass of each sample was quantified as WSOA = WSOC × (OM:OC), with WSOC measured on the same filter by a TOC analyser and OM:OC obtained from the offline-AMS elemental analysis; each PMF factor was then placed on an atmospheric water-soluble mass basis by scaling this total WSOA by its fractional contribution to the offline organic signal (WSOC:OC = 0.64, range 0.52–0.74; Table S1). No factor-specific Daellenbach recoveries were applied.

Table S1. Offline-AMS extraction and water-soluble OA quantification. The water-soluble organic aerosol mass was anchored to WSOC (TOC analyser) via WSOA = WSOC × (OM:OC) from the offline-AMS elemental analysis; no factor-specific Daellenbach recoveries were applied.

Quantity	Value	Source / note
Extraction (punches, area, water vol., time, T)	47 mm-diameter filter section cut into pieces; 20 mL Milli-Q water (18.2 MΩ cm, TOC < 5 ppb); 30 min	this study; per Daellenbach 2016

Quantity	Value	Source / note
	sonication in an ice-water bath; 0.45 µm syringe filter	
Nebuliser / carrier gas	TSI Model 3076 constant-output atomiser / Ar (≥ 99.999 %)	Bozzetti 2017 (Ar)
WSOC:OC (median, IQR)	0.64 (IQR 0.52–0.74; n = 428)	this study
WSOC (water-soluble OC)	measured on the same 24 h filter with a TOC analyser	this study
OM:OC (offline-AMS)	per filter, Improved-Ambient elemental analysis of the water-soluble mass spectrum	this study (Canagaratna 2015)
Water-soluble OA mass (WSOA)	WSOA = WSOC × (OM:OC); each PMF factor scaled by its fractional contribution to the offline organic signal	this study
Field / extraction blanks	processed and subtracted identically	subtracted

S1.3 Number of factors in the offline PMF solution

The offline PMF was run on the water-soluble high-resolution mass spectra (one per 24 h filter) and the three-, four- and five-factor solutions were compared. No Q/Qexp, fPeak, bootstrap or f_{43}/f_{44} diagnostics are reported for the offline solution; the quantitative PMF diagnostics presented in this Supplement (Fig. S2) apply to the online solution only. The offline factor number was instead selected on the interpretability of the factor mass spectra and on their independent correspondence with the online factors.

In the three-factor solution LO-OOA and MO-OOA merged into a single oxygenated factor of intermediate oxidation state, which correlated only weakly with either the reduced-nitrogen fragments or sulfate. Because the online–offline comparison in Sect. 3.3 rests on the contrast between the less- and more-oxidised secondary factors, this solution was rejected.

In the five-factor solution the additional factor arose from factor splitting rather than from the resolution of a new source: the two daughter factors had closely similar mass spectra and strongly correlated time series, and neither carried a distinguishing tracer, diurnal cycle or source signature.

The four-factor solution is the smallest one in which every factor is separately interpretable and finds an independent counterpart in the online apportionment: the combined primary/POA factor tracks the hydrocarbon fragments and the summed online HOA + COA mass, BBOA the biomass-burning fragment

$C_2H_4O_2^+$, LO-OOA the reduced-nitrogen fragments, and MO-OOA the CO_2^+ fragment and sulfate. Each factor also corresponds to an independently measured tracer not used in the apportionment (BBOA with levoglucosan and K^+, primary/POA with EC, and the oxygenated factors with WSOC and sulfate; Table S2).

S1.4 PMF and online vs. offline factor correspondence

Online and offline PMF were run independently using PMF2, following the group's AMS factor-analysis procedures (Ulbrich et al., 2009; Zhang et al., 2011a); the offline solution is an unconstrained PMF2 on the offline-AMS matrix (40 filters × m/z) resolving four water-soluble factors, with no a priori profiles. Factors were matched a posteriori by spectral similarity (Table S2) and time-series correlation (Fig. S8). MO-OOA online and offline correlate at r = 0.93 (R^2 = 0.86) over the 40 paired filter days (27 with a valid online–offline MO-OOA pair), and their major mass-spectral peaks agree, establishing them as the same factor. The two platforms also agree at the bulk level (Fig. S4): the 24 h-averaged online PM_1 OC and OA track the offline $PM_{2.5}$ OC and OA (r^2 = 0.88 and 0.89; slopes 0.85 and 0.86), PM_1 OA tracks $PM_{2.5}$ WSOA (r^2 = 0.84), and the online 370 nm BrC absorption correlates with the offline methanol-soluble 365 nm absorption (r^2 = 0.70, slope 0.72) far more closely than with the water-soluble absorption (r^2 = 0.25) — an online↔offline validation that also localises the discrepancy to the water-soluble extraction window rather than to the sampling or the instruments.

(a) Five-factor solution

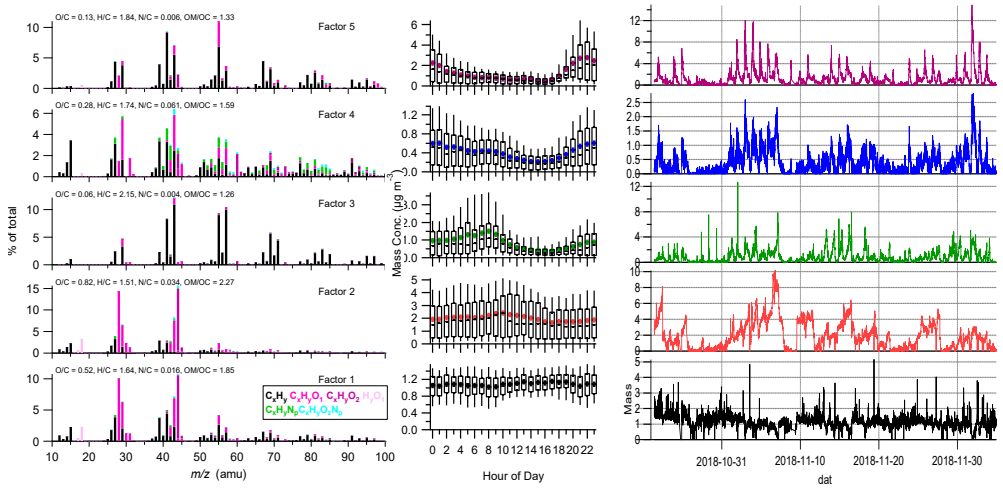

(b) Six-factor solution (adopted)

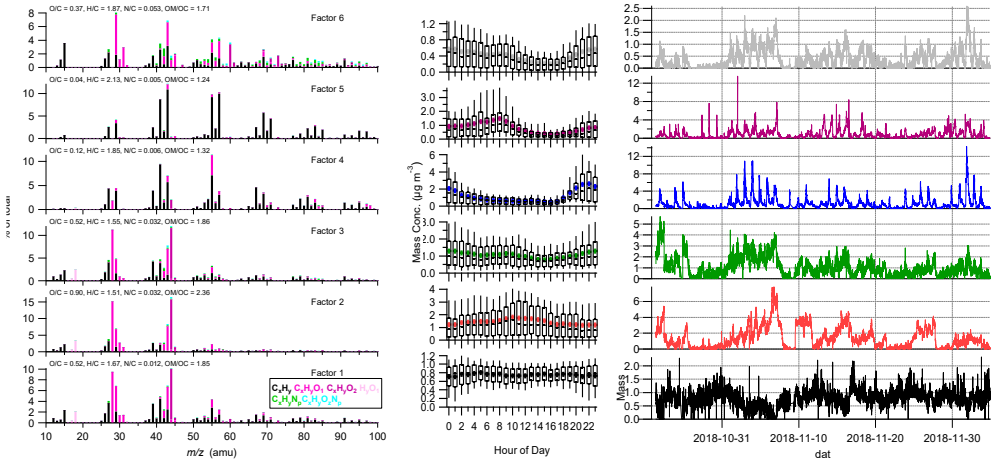

(c) Seven-factor solution

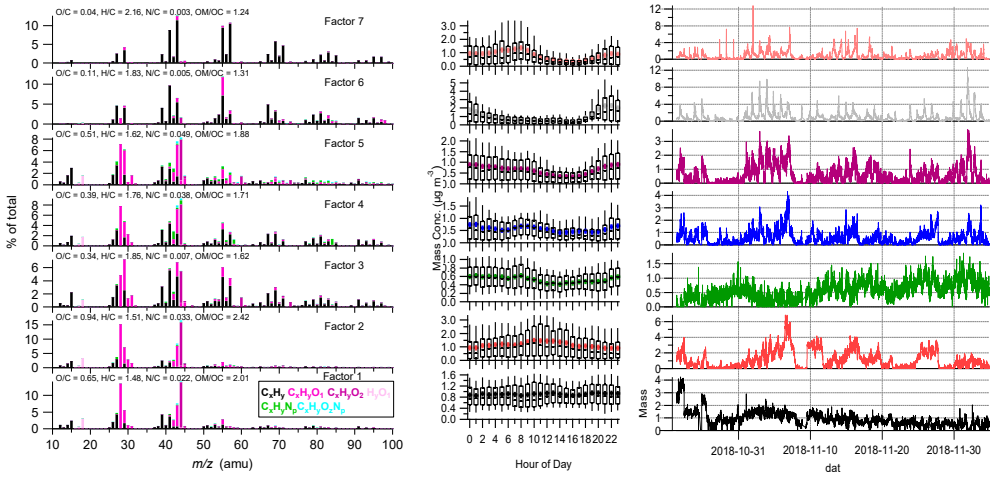

Fig. S1. Selection of the six-factor online PMF solution. Factor high-resolution mass spectra (coloured by ion family: C_xH_y, $C_xH_yO_1$, $C_xH_yO_2$, H_yO_1, $C_xH_yN_p$, $C_xH_yO_zN_p$; elemental ratios annotated) and the corresponding factor mass-concentration time series for the (a) five-, (b) six- and (c) seven-factor solutions of the online PM_1 HR-ToF-AMS dataset (2018 winter campaign, 23 Oct–4 Dec 2018). (a) At five factors the two less-oxidised secondary factors are not separated: a single LO-OOA carries both the reduced-nitrogen and the daytime-photochemical signatures, so the nighttime and daytime secondary material cannot be distinguished. (b) Six factors resolve, in order of oxidation state, Factor 5 (O/C 0.04, H/C 2.13) — HOA; Factor 4 (O/C 0.12) — COA; Factor 3 (O/C 0.52, N/C 0.032) — BBOA; Factor 1 (O/C 0.52) and Factor 6 (O/C 0.37, N/C 0.053) — the two less-oxidised secondary factors LO-OOA1 and LO-OOA2; and Factor 2 (O/C 0.90, OM:OC 2.36) — MO-OOA, each with a distinct mass spectrum, time series and diurnal behaviour. (c) The seventh factor does not isolate an additional source: it splits an existing oxygenated factor into two components with closely similar spectra and correlated time series, and carries no distinguishing tracer. The six-factor solution was therefore retained; its Q/Qexp, fPeak and explained-variation diagnostics are given in Fig. S2, and the offline factor spectra used for the online↔offline matching are compared factor-by-factor in Table S2, with the corresponding factor time series in Fig. S8.

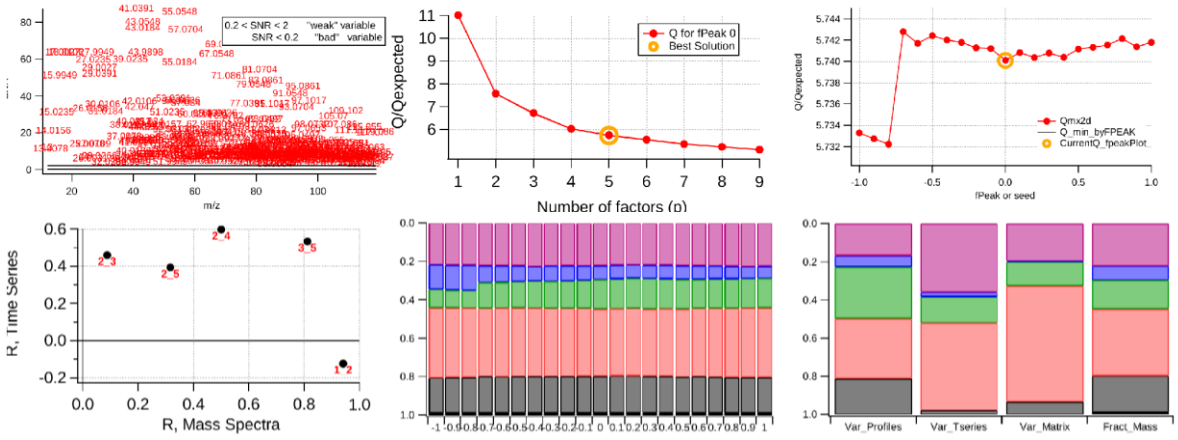

Fig. S2. PMF solution diagnostics for the online dataset. SNR classifies each m/z as strong, weak (0.2 < SNR < 2) or bad (SNR < 0.2). Q/Qexpected decreases smoothly with the number of factors p; the six-factor solution was retained because it isolates a physically-distinct factor beyond the statistical knee while keeping Q/Qexp near unity. Q versus fPeak (seed) is flat and shallow around fPeak = 0 (rotational stability), and the R(time series) vs R(mass spectra) map plus the explained-variation breakdown (Var_Profiles, Var_Tseries, Var_Matrix, Fract_Mass across fPeak) show the solution is robust to rotation.

Table S2. Online↔offline factor correspondence: pairwise mass-spectral R^2 between each offline factor (rows) and each online factor (columns). The matched MO-OOA pair gives $R^2 = 0.81$. Because AMS unit-mass OA spectra are broadly similar, off-diagonal spectral R^2 are also high; the one-to-one factor mapping is therefore established primarily by the mass-concentration time-series correspondence (Fig. S8, S5), with this spectral matrix providing supporting consistency.

offline ╲ online	**HOA/POA**	**BBOA**	**LO-OOA**	**MO-OOA**
POA	0.28	0.91	0.70	0.86
BBOA	0.24	0.94	0.70	0.86
LO-OOA	0.14	0.71	0.72	0.76
MO-OOA	0.05	0.70	0.42	0.81

The offline PMF solution is resolved from a small matrix (40 filters × m/z), so its stability warrants explicit attention. Two independent lines of evidence indicate the four-factor offline solution is robust: each offline factor matches an online counterpart in its high-resolution mass spectrum (Table S2), and the offline MO-OOA time series reproduces the 24 h-averaged online MO-OOA at $r = 0.93$ ($R^2 = 0.86$; Fig. S5) even though the two solutions were obtained independently — a convergence a rotationally-unstable solution could not produce.

(a) Three-factor solution

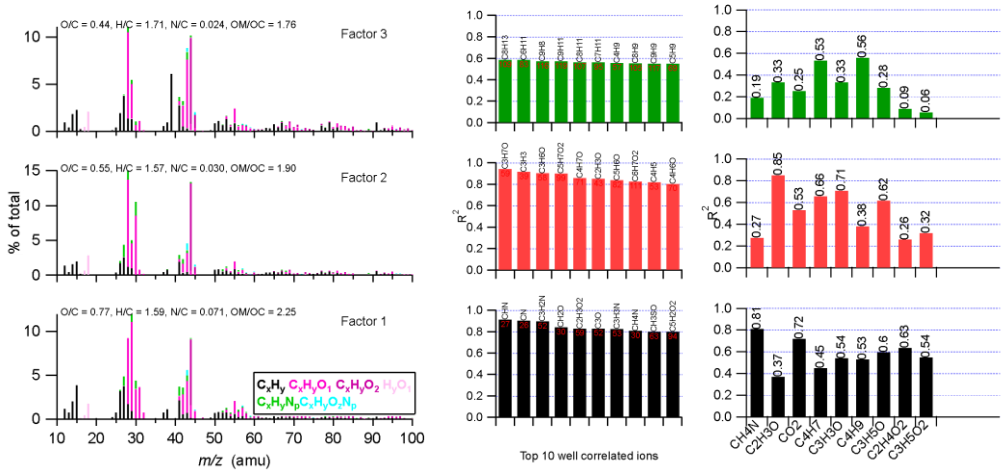

(b) Four-factor solution (adopted)

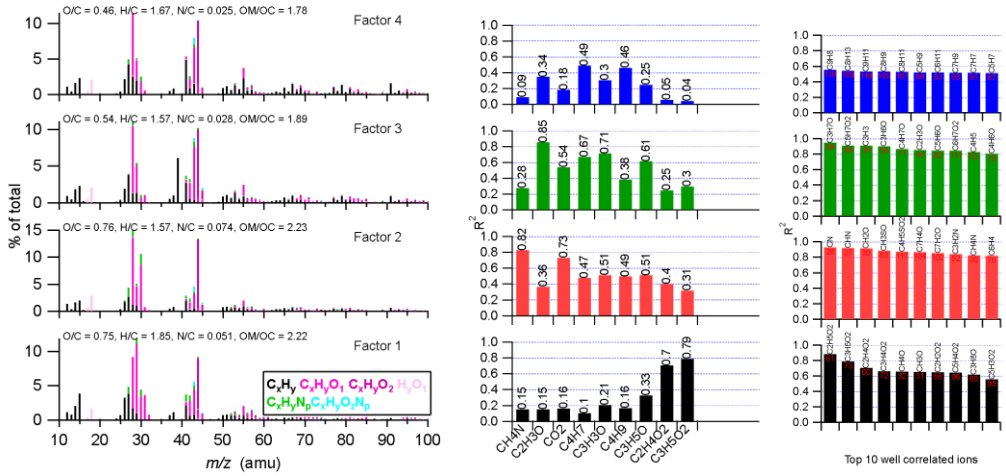

(c) Five-factor solution

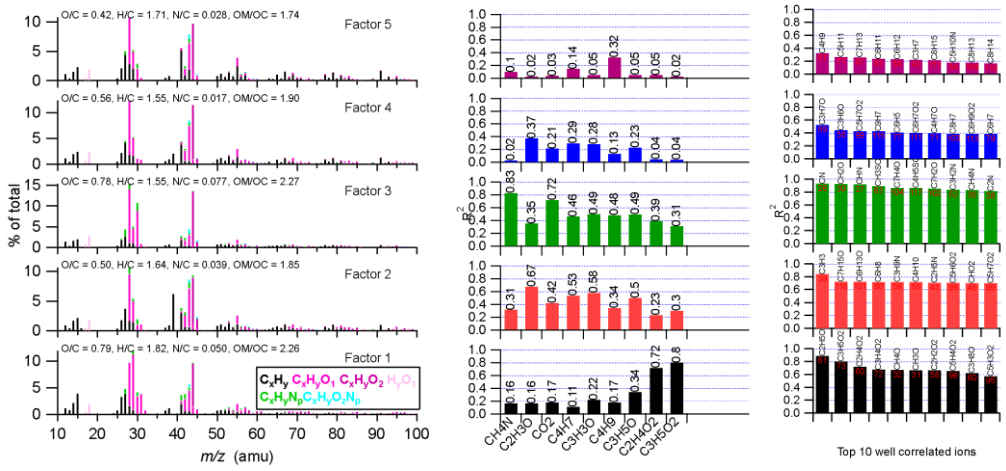

Fig. S3. Selection of the four-factor offline PMF solution. High-resolution mass spectra of the water-soluble factors resolved by the (a) three-, (b) four- (adopted) and (c) five-factor solutions. At three factors LO-OOA and MO-OOA merge into a single oxygenated factor of intermediate oxidation state; at five factors the additional factor arises from splitting, the two daughter factors having closely similar spectra and strongly correlated time series with no distinguishing tracer or diurnal signature. Quantitative PMF diagnostics (Q/Qexp versus factor number, rotational stability versus fPeak) are reported for the online solution only (Fig. S2).

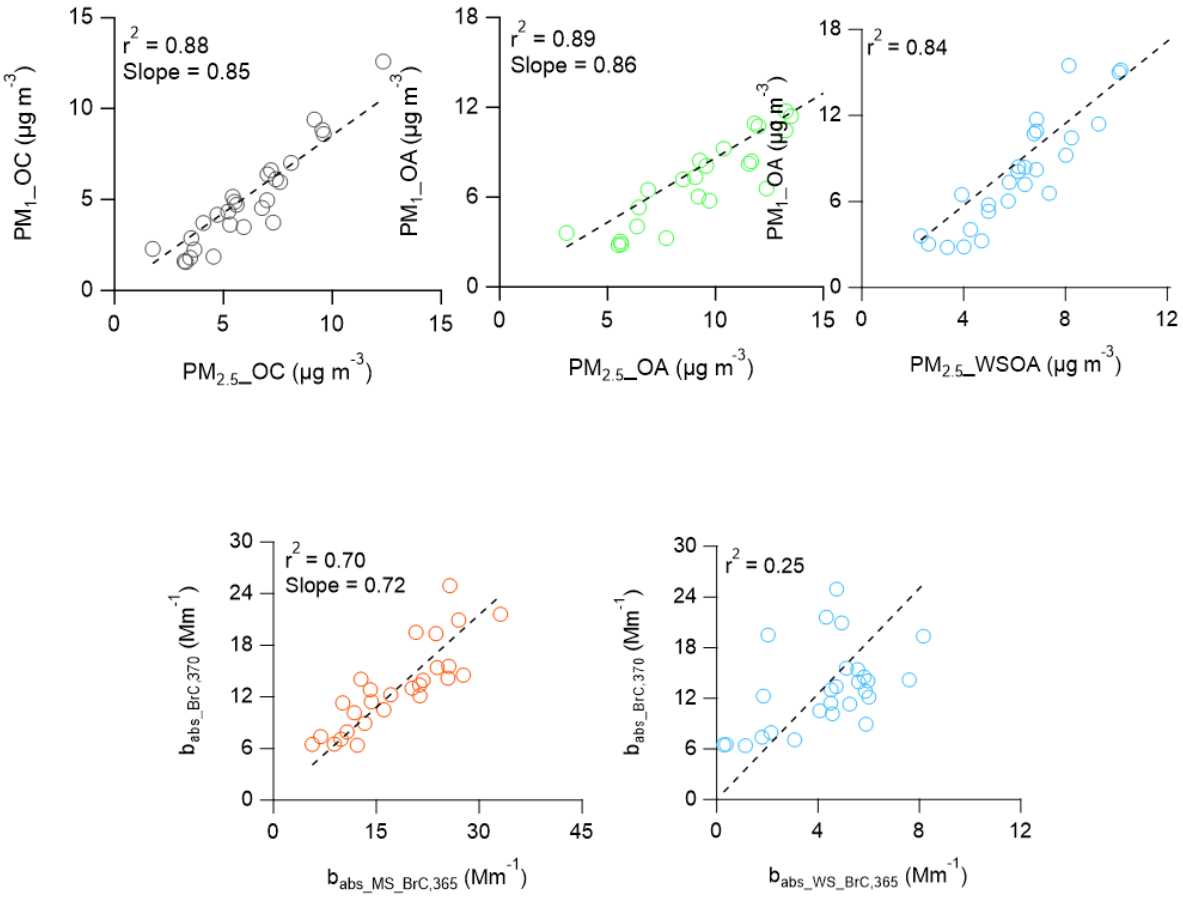

Fig. S4. Online–offline measurement validation. (Top) 24 h-averaged online PM_1 species versus the co-located offline $PM_{2.5}$ filter measurements: PM_1_OC vs $PM_{2.5}$_OC (r^2 = 0.88, slope = 0.85), PM_1_OA vs $PM_{2.5}$_OA (r^2 = 0.89, slope = 0.86) and PM_1_OA vs $PM_{2.5}$_WSOA (r^2 = 0.84). (Bottom) Online aethalometer BrC absorption at 370 nm versus the offline solvent-extract BrC absorption at 365 nm, for the methanol-soluble (babs_MS_BrC,365; r^2 = 0.70, slope = 0.72) and the water-soluble (babs_WS_BrC,365; r^2 = 0.25) extracts. Each open circle is one paired filter day; dashed lines are the orthogonal-distance-regression fits. The close mass agreement and the strong methanol-soluble absorption correspondence show

that the two platforms sample the same aerosol, whereas the weak water-soluble correspondence indicates that the offline water extraction recovers only part of the absorbing material — the measurement-window effect discussed in the main text.

S2 Attribution of BrC absorption and its robustness

S2.1 Regression, uncertainties and collinearity

Source-resolved MAC were obtained by multiple linear regression of $b_{abs,BrC}$ onto the PMF factor mass time series, identically for the online and offline platforms. We report bootstrap 95 % confidence intervals, per-factor variance-inflation factors (VIF) and the factor-matrix condition number, and a non-negative least-squares (NNLS) refit that pins the slightly negative offline LO-OOA coefficient at zero (Table S3).

Table S3. Source-resolved mass absorption cross-sections (MAC, $m^2\ g^{-1}$) of the PMF factors, with bootstrap uncertainty and collinearity diagnostics. VIF is the per-factor variance-inflation factor of the factor matrix used as regressors; NNLS is the coefficient obtained when the fit is constrained to non-negative values.

Factor	Online MAC (95 % CI)	Offline MAC (95 % CI)	VIF	NNLS
HOA / POA	0.65 [0.54, 0.76]	0.61 [0.40, 0.80]	2.0	0.54
BBOA	5.66 [5.26, 6.05]	0.64 [0.37, 0.99]	3.3	0.62
LO-OOA1 / LO-OOA	4.22 [4.12, 4.32]	−0.13 [−0.26, 0.01] (comb.)	1.2	0.00
LO-OOA2	2.94 [2.75, 3.13]	—	2.0	—
MO-OOA	0.07 [0.01, 0.15]	0.88 [0.71, 1.04]	1.6	0.85

Bootstrap 95 % confidence intervals are from 2000 resamples. The condition number of the factor matrix — the ratio of its largest to its smallest singular value, a measure of how strongly the factor time series co-vary as regressors — is 12.0 for the online solution and 4.6 for the offline solution; values below about 10 indicate weak collinearity and 10–30 moderate collinearity, so neither regression is dominated by it. The bootstrap intervals separate every online factor from zero, so the online source ranking is statistically robust. The unconstrained offline LO-OOA coefficient is slightly negative (−0.13 $m^2\ g^{-1}$; 95 % CI [−0.26, 0.01]) and is therefore indistinguishable from zero rather than evidence of physical negative absorption; the non-negative least-squares refit pins it at 0.00 $m^2\ g^{-1}$, leaves MO-OOA dominant offline (unconstrained 0.88, non-negative least-squares 0.85 $m^2\ g^{-1}$) and leaves the online source ranking unchanged. This is what the solubility argument predicts: once the dominant water-soluble MO-OOA absorption is accounted for, LO-OOA carries no separable water-soluble absorption.

S2.2 Sensitivity to the black-carbon correction

Table S4. Sensitivity of the 370 nm BrC fraction and the online source ranking to the black-carbon correction. The BrC fraction is recomputed for AAE_BC = 0.9, 1.0, 1.1 and BC reference bands of 880 and 950 nm. At AAE_BC = 1.0 the two reference bands give an identical BrC fraction by construction (a pure-BC spectrum with AAE = 1.0 extrapolates to the same 370 nm value from either band). Varying AAE_BC over 0.9–1.1 changes the campaign-mean BrC fraction by about ±6–7 % absolute; the source ranking (regression MAC order) is unchanged in every case because the BC correction rescales $b_{abs,BrC}$ without altering the relative factor loadings.

AAE_BC / reference band	BrC fraction at 370 nm	Source ranking
1.0 / 880 nm (base)	25.7 %	BBOA > LO-OOA1 > LO-OOA2 > HOA > MO-OOA
1.0 / 950 nm	25.7 %	unchanged
0.9 / 880 nm	31.8 %	unchanged
0.9 / 950 nm	32.4 %	unchanged
1.1 / 880 nm	19.0 %	unchanged
1.1 / 950 nm	18.4 %	unchanged

S3 Supporting composition and optical results

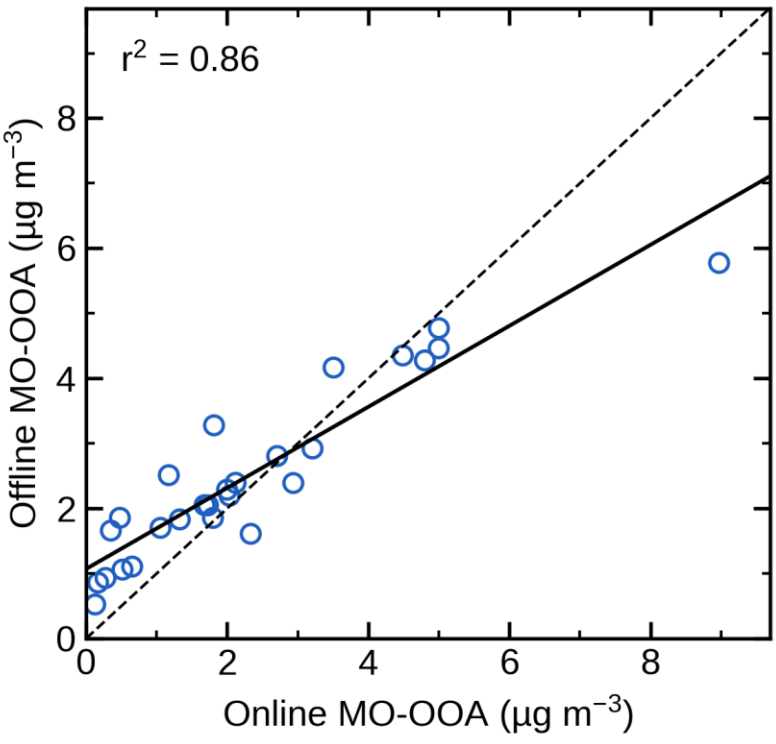

Fig. S5. Online versus offline MO-OOA mass-concentration correspondence. Each open circle is one of the n = 27 paired filter days (of 40) for which both the time-resolved online AMS (24 h-averaged) and the offline-AMS PMF resolved an MO-OOA factor; the two agree at r = 0.93 (r^2 = 0.86). The dashed line is 1:1 and the solid line is the orthogonal-distance-regression fit. This independent quantitative agreement, together with the mass-spectral match (Table S2), establishes that the online whole-particle MO-OOA and the offline water-soluble MO-OOA are the same atmospheric factor rather than two coincidentally-named PMF outputs.

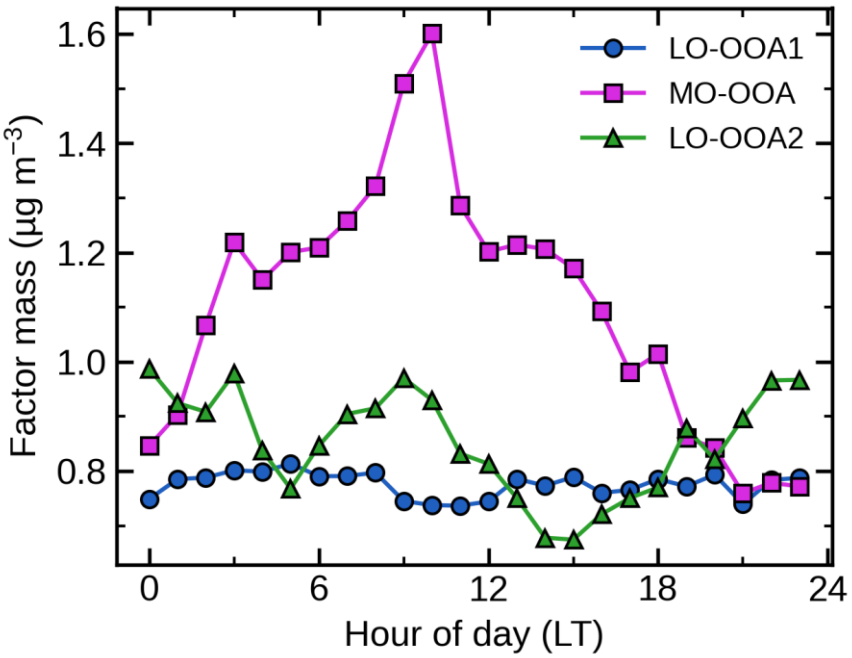

Fig. S6. Mean diurnal cycles of the secondary OA factors (local time). MO-OOA (magenta squares) peaks in the mid-morning (~09–10 LT), consistent with photochemical secondary formation and the daytime photobleaching window discussed in the main text; LO-OOA1 (blue circles) is nearly flat, and LO-OOA2 (green triangles) shows a weaker mid-morning rise and an evening recovery. Points are hour-of-day averages over the campaign; the morning MO-OOA maximum is the feature that co-locates with the daytime decline in mass-normalised BrC absorption (Sect. 3.2.3).

m/z	Chemical formula	Proposed structures
26	CN^+	---
27	CHN^+	---
29	CH_3N^+	---
30	CH_4N^+	---
40	$C_2H_2N^+$	---
41#	$C_2H_3N^+$	---
46#	CH_4NO^+	---
57#	$C_2H_3NO^+$	
68#	$C_3H_4N_2^+$	
69#	$C_3H_3NO^+$	
74	$C_2H_6N_2O^+$	
96#	$C_4H_4N_2O^+$	

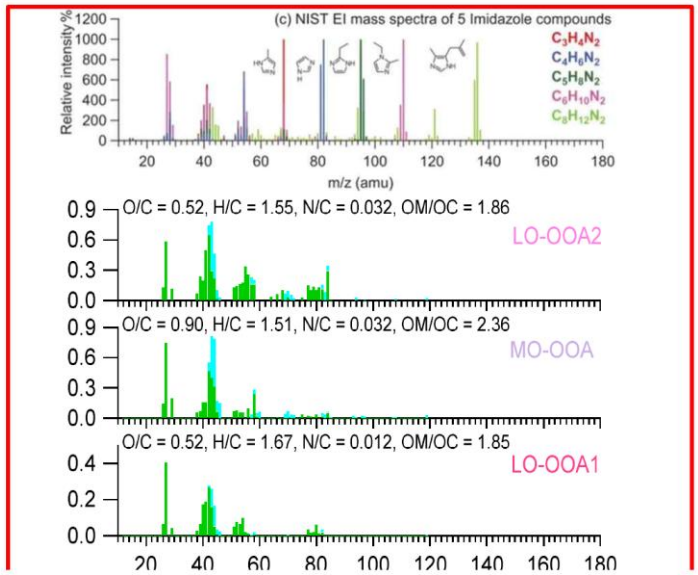

Fig. S7. Reduced-nitrogen (imidazole-type) chromophores in the online factors. (Left) High-resolution AMS fragments consistent with imidazole/N-heterocycle chemistry (m/z, assigned formula and candidate structures); several — e.g. $C_3H_4N_2^+$ at m/z 68 and $C_4H_4N_2O^+$ at m/z 96 — are known products of aqueous glyoxal reactions with reduced nitrogen (NH_4^+/amines). (Right) NIST EI reference spectra of five imidazole compounds (top) compared with the measured high-resolution spectra of LO-OOA2, MO-OOA and LO-OOA1 (elemental ratios annotated); the reduced-nitrogen fragment pattern is expressed most strongly in the nighttime secondary factor LO-OOA2. Data: this campaign; reference spectra from NIST.

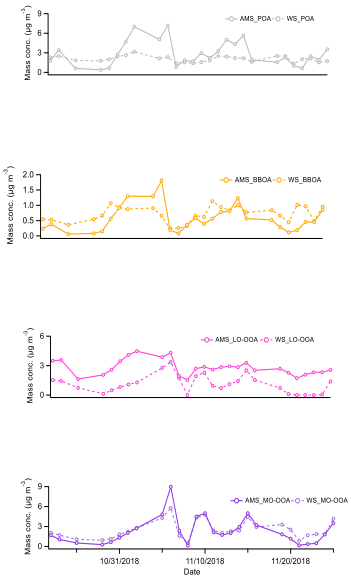

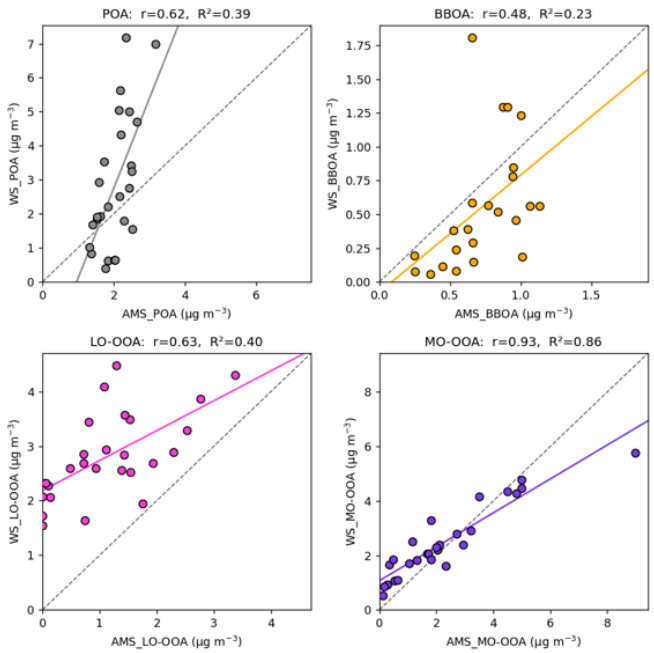

Fig. S8. Online–offline factor time-series comparison. Time series of the four offline water-soluble PMF factors (primary OA, BBOA, LO-OOA, MO-OOA; one value per 24 h filter) overlaid on the corresponding 24 h-averaged online AMS factors, one panel per factor pair. Each pair follows the same day-to-day variation; together with the mass-spectral correspondence in Table S2 this establishes the one-to-one mapping between the online and offline solutions used in Sect. 3.3. The offline factor mass spectra are shown in Fig. S3b and the bulk PM1 OA versus PM2.5 WSOA comparison in Fig. S4.

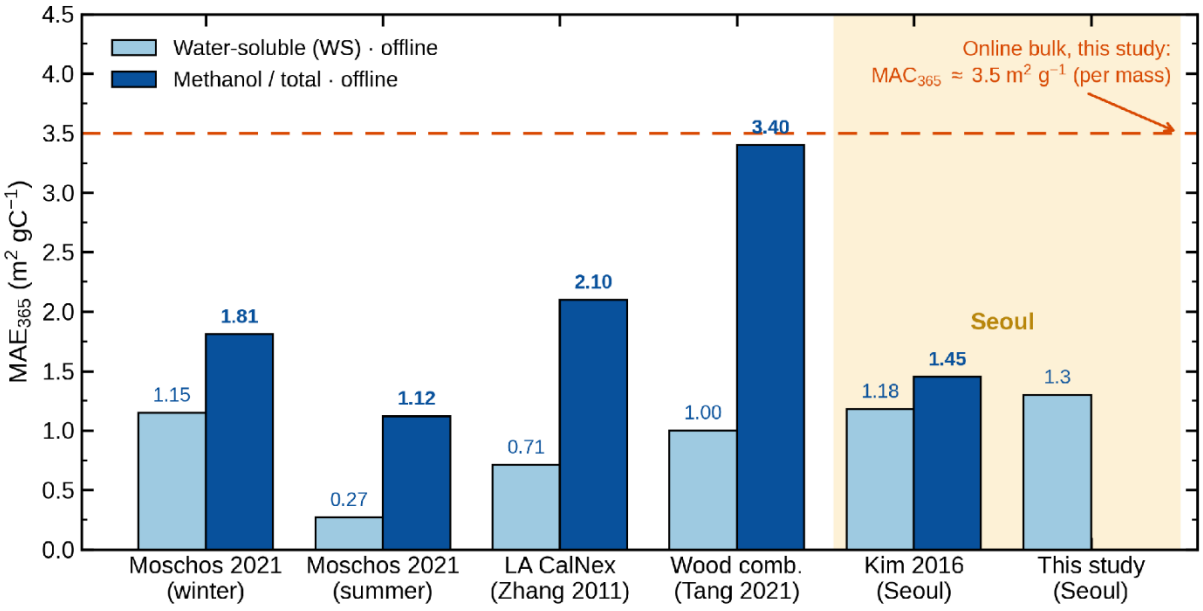

Fig. S9. The offline water-soluble MAE of this study reproduces the earlier Seoul record and the water-soluble BrC literature. Bars show the mass absorption efficiency at 365 nm (MAE_{365}, per carbon mass, m^2 gC^{-1}) for water-soluble (light blue) and methanol/total (dark blue) extracts from Moschos et al. (2021, winter and summer), Zhang et al. (2011b; LA CalNex), Tang et al. (2021; wood combustion), the earlier Seoul offline record (Kim et al., 2016) and this study (water-soluble only; methanol extracts were not used here). This study's offline WS MAE_{365} (~1.3 m^2 gC^{-1}) falls within the literature range and matches Kim et al. (2016; 1.18). The online whole-particle bulk MAC_{365} of this study (~3.5 m^2 g^{-1}, per mass; dashed orange line) is shown separately because it uses a different normalization (per total aerosol mass rather than per carbon) and captures the whole particle, not only the water-soluble fraction, and is therefore not directly comparable as a bar height.

Table S5. Reported OA source-apportionment mass fractions (% of total OA) used to derive the compiled single-site contributions to BrC absorption in main-text Table 2 (Option-B weighting by this study's measured factor MACs). Factors are grouped as combustion (biomass-burning BBOA and coal-combustion CCOA), other primary (HOA, COA), less-oxidized secondary (LO-OOA/SV-OOA) and more-oxidized secondary (MO-OOA/LV-OOA). Values are from the cited studies for the indicated season; Seoul and the Wang et al. (2022) winter-China rows are apportioned directly on an absorption basis and are not re-weighted.

Site	Season	Combustion (BBOA/CCOA)	Other primary (HOA/COA)	Less-ox. sec. (LO/SV-OOA)	More-ox. sec. (MO/LV-OOA)	Reference
Shanghai, China	late spring	0	24.0	46.8	29.2	Huang et al. (2012)
Hong Kong	winter	0	19.1	26.0	54.8	Li et al. (2015)

Site	Season	Combustion (BBOA/CCOA)	Other primary (HOA/COA)	Less-ox. sec. (LO/SV-OOA)	More-ox. sec. (MO/LV-OOA)	Reference
Lanzhou, China	winter	32.8 (CCOA 22.0, BBOA 10.8)	30.0	22.3	14.9	Xu et al. (2016)
Barcelona, Spain	winter	11 (BBOA)	33	27	28	Mohr et al. (2012)
Helsinki, Finland	spring	14 (BBOA)	16	20	51	Crippa et al. (2014)
Paris, France	winter	14 (BBOA)	29	28.5*	28.5*	Crippa et al. (2013)
Singapore	tropical	0	57.5 (HOA 19.4, O-HOA 26.4, COA 11.7)	10.4	32.1	Kasthuriarachchi et al. (2020)
SE USA (Centreville)	summer	10 (BBOA)	0	33	39‡	Xu et al. (2015)

* Paris OOA reported as a single combined factor (57 %); split 50:50 between less- and more-oxidized for the Option-B weighting.

‡ Centreville also resolves Isoprene-OA (18 % of OA; biogenic SOA), treated as optically weak (MAC 0.08) in the Option-B weighting.

S4 Recommended control experiments (to separate prep-formed from atmospheric water-soluble N)

The strongest single addition to the argument would be a control that isolates the preparation-formed reduced-nitrogen chromophores (branch b, Sect. 3.3.3) from real atmospheric water-soluble N surfaced offline (branch a). Any of the following, even at small scale, would do so:

- Argon vs air nebulisation of the same extract: air enables an oxidative browning pathway that Ar suppresses; a difference isolates that pathway and confirms Ar removes it.
- Standing-time / concentration test: measure absorbance and reduced-N fragments as a function of extract standing time and concentration; prep-formed chromophores grow with residence time and concentration.
- Spike test: add a known carbonyl (glyoxal/methylglyoxal) + amine/ammonium mixture to a blank extract and quantify the reduced-N chromophore yield under the same nebulisation/drying.

References (Supplement)

Bozzetti, C., et al.: Argon offline-AMS source apportionment of organic aerosol over yearly cycles for an urban, rural, and marine site in northern Europe, Atmos. Chem. Phys., 17, 117–141, https://doi.org/10.5194/acp-17-117-2017, 2017.

Canagaratna, M. R., et al.: Elemental ratio measurements of organic compounds using aerosol mass spectrometry, Atmos. Chem. Phys., 15, 253–272, https://doi.org/10.5194/acp-15-253-2015, 2015.

Canonaco, F., et al.: SoFi, an IGOR-based interface for the efficient use of the generalized multilinear engine (ME-2)…, Atmos. Meas. Tech., 6, 3649–3661, https://doi.org/10.5194/amt-6-3649-2013, 2013.

Daellenbach, K. R., et al.: Characterization and source apportionment of organic aerosol using offline aerosol mass spectrometry, Atmos. Meas. Tech., 9, 23–39, https://doi.org/10.5194/amt-9-23-2016, 2016.

Kim, H., Zhang, Q., Bae, G.-N., Kim, J. Y., and Lee, S. B.: Sources and atmospheric processing of winter aerosols in Seoul, Korea: insights from real-time measurements using a high-resolution aerosol mass spectrometer, Atmos. Chem. Phys., 17, 2009–2033, https://doi.org/10.5194/acp-17-2009-2017, 2017.

Middlebrook, A. M., Bahreini, R., Jimenez, J. L., and Canagaratna, M. R.: Real-time measurement of aerosol particle collection efficiency using ambient data from the Aerodyne aerosol mass spectrometer, Aerosol Sci. Technol., 46, 258–271, https://doi.org/10.1080/02786826.2011.620041, 2012.

Paatero, P. and Tapper, U.: Positive matrix factorization…, Environmetrics, 5, 111–126, https://doi.org/10.1002/env.3170050203, 1994.

Ulbrich, I. M., et al.: Interpretation of organic components from Positive Matrix Factorization of aerosol mass spectrometric data, Atmos. Chem. Phys., 9, 2891–2918, https://doi.org/10.5194/acp-9-2891-2009, 2009.

Zhang, Q., Jimenez, J. L., Canagaratna, M. R., Ulbrich, I. M., Ng, N. L., Worsnop, D. R., and Sun, Y.: Understanding atmospheric organic aerosols via factor analysis of aerosol mass spectrometry: a review, Anal. Bioanal. Chem., 401, 3045–3067, https://doi.org/10.1007/s00216-011-5355-y, 2011a.

Zhang, X., Lin, Y.-H., Surratt, J. D., Zotter, P., Prévôt, A. S. H., and Weber, R. J.: Light-absorbing soluble organic aerosol in Los Angeles and Atlanta: A contrast in secondary organic aerosol, Geophys. Res. Lett., 38, L21810, https://doi.org/10.1029/2011GL049385, 2011b.